

# Bayesian analysis of the hardening in AMS-02 nuclei spectra

Jia-Shu Niu,<sup>1,2,\*</sup> Tianjun Li,<sup>2,†</sup> and Hui-Fang Xue<sup>3</sup>

<sup>1</sup>*Institute of Theoretical Physics, Shanxi University, Taiyuan, 030006, China*

<sup>2</sup>*CAS Key Laboratory of Theoretical Physics, Institute of Theoretical Physics, Chinese Academy of Sciences, Beijing, 100190, China*

<sup>3</sup>*Astronomy Department, Beijing Normal University, Beijing 100875, China*

(Dated: May 28, 2022)

Based on the precision nuclei data released by AMS-02, the spectra hardening of both the primary (proton, helium, carbon, and oxygen) and the secondary (anti-proton, lithium, beryllium, and boron) cosmic ray (CR) nuclei have been studied in this work. With the diffusion-reacceleration model, we use 2 schemes to reproduce the hardening in the spectra: (i) adding a high-rigidity break in primary source injection; (ii) adding a high-rigidity break in diffusion coefficient. The global fitting results show that both schemes could reproduce the spectra hardening in current status. More multi-TV data is needed if one wants to distinguish these two schemes. In our global fitting, each of the nuclei species is allocated a independent solar modulation potential and a re-scale factor (which accounts for the isotopic abundance for primary nuclei and production cross section for secondary nuclei). The fitted values of these two parameter classes show us some hints on some new directions in CR physics. Particularly, it shows that beryllium has the specificity not only on its propagation in heliosphere, but also on the production cross section and isotopic abundance. This may be related to some problems in stellar physics and cosmology on this special element.

## I. INTRODUCTION

Understanding the spectral features in cosmic rays (CRs) is of fundamental importance for studying their origin and propagation. Great progress in cosmic ray (CR) spectrum measurement has been made in recent years with new a generation of space-borne and ground-based experiments in operation. The fine structure of spectral hardening for primary nuclei at  $\sim 300$  GV was observed by ATIC-2 [1], CREAM [2], PAMELA [3], and AMS-02 [4, 5].

Recently, AMS-02 has released the energy spectra of He, C, and O [6], which confirms the spectral hardening of the CR primary nuclei. Moreover, the subsequently released energy spectra of Li, Be, and B [7] show that the secondary nuclei spectra hardens even more than that of the primary ones at a few hundred GV. Because the secondary CR particles are produced in collisions of primary CR particles with interstellar medium (ISM), combining these data together would provide us a excellent opportunity to study the hardening of the CR nuclei spectra quantitatively.

Some previous works has proposed different solutions to this problem: (i) adding a new break in high-energy region ( $\sim 300$  GV) to the injection spectra (see, e.g., [8–12]); (ii) adding a new in high-rigidity break to the diffusion coefficient (see, e.g., [13]); (iii) inhomogeneous diffusion (see, e.g., [14–19]); (iv) the superposition of local and distant sources (see, e.g., [20–23]).

In this work, we do a global fitting on these primary and secondary nuclei spectra from AMS-02. Two

schemes are considered: (i) the hardening of the spectra comes from the source – a new high-rigidity break is added in the primary source injections (Scheme I); (ii) the hardening of the spectra comes from the propagation – a new high-rigidity break is added in the diffusion coefficient (Scheme II). We hope that the precise spectra data from AMS-02 would give us a clear result, at least a tendency.

The paper is organized as follows. We first list the setups in Sec. II. The fitting results is give in Sec. III. Then we present some discussions and conclusions in Sec. IV.

## II. SETUPS

In this section, we list some of the most important setups in this work, more detailed similar configurations could be found in Niu and Li [24].

### A. Model

As in our previous work [10, 24], we use separate primary source spectra settings for proton and other nuclei species because of the significant difference observed in the slopes of proton and other nuclei species when  $Z > 1$ .

#### 1. Propagation Model

The diffusion-reacceleration model is used in the global fitting, which is widely used and can give a consistent fitting results to the AMS-02 nuclei data (see, e.g., [24–26]).  $v_A$  is used to characterize the reacceleration, and  $z_h$  represents the half-height of the propagation region in

---

\* jsniu@sxu.edu.cn

† tli@itp.ac.cn

the galaxy for the cylindrical coordinate system. In the whole propagation region, a uniform diffusion coefficient is used which depends on CR particles' rigidity.

In Scheme I, the diffusion coefficient is parametrized as

$$D_{xx}(R) = D_0 \beta \left( \frac{R}{R_0} \right)^\delta, \quad (1)$$

where  $\beta$  is the velocity of the particle in unit of light speed  $c$ ,  $R_0$  is the reference rigidity, and  $R \equiv pc/Ze$  is the rigidity.

For Scheme II, the diffusion coefficient is parametrized as

$$D_{xx}(R) = D_0 \cdot \beta \left( \frac{R_{\text{br}}}{R_0} \right) \times \begin{cases} \left( \frac{R}{R_{\text{br}}} \right)^{\delta_1} & R \leq R_{\text{br}} \\ \left( \frac{R}{R_{\text{br}}} \right)^{\delta_2} & R > R_{\text{br}} \end{cases}, \quad (2)$$

where  $R_{\text{br}}$  is the high-rigidity break;  $\delta_1$  and  $\delta_2$  are the diffusion slopes below and above the break.

## 2. Primary Sources

The primary source injection spectra of all kinds of nuclei are assumed to be a broken power law form. In Scheme I, it is represented as:

$$q_i = N_i \times \begin{cases} \left( \frac{R}{R_{A1}} \right)^{-\nu_{A1}} & R \leq R_{A1} \\ \left( \frac{R}{R_{A1}} \right)^{-\nu_{A2}} & R_{A1} < R \leq R_{A2} \\ \left( \frac{R}{R_{A2}} \right)^{-\nu_{A3}} \left( \frac{R_{A2}}{R_{A1}} \right)^{-\nu_{A2}} & R > R_{A2} \end{cases}, \quad (3)$$

where  $i$  denotes the species of nuclei,  $N_i$  is the normalization constant proportional to the relative abundance of the corresponding nuclei, and  $\nu_A = \nu_{A1}(\nu_{A2}, \nu_{A3})$  for the nucleus rigidity  $R$  in the region divided by two reference rigidity  $R_{A1}$  and  $R_{A2}$ . In this work, we use independent proton injection spectrum, and the corresponding parameters are  $R_{p1}$ ,  $R_{p2}$ ,  $\nu_{p1}$ ,  $\nu_{p2}$ , and  $\nu_{p3}$ . All the  $Z > 1$  nuclei are assumed to have the same value of injection parameters.

For Scheme II, we have

$$q_i = N_i \times \begin{cases} \left( \frac{R}{R_A} \right)^{-\nu_{A1}} & R \leq R_A \\ \left( \frac{R}{R_A} \right)^{-\nu_{A2}} & R > R_A \end{cases}, \quad (4)$$

which are described by one break at the rigidity  $R_A$  ( $R_p$ ) and two slopes below ( $\nu_{A1}$  or  $\nu_{p1}$ ) and above ( $\nu_{A2}$  or  $\nu_{p2}$ ) it.

## 3. Solar modulation

We adopt the force-field approximation [27] to describe the effects of solar modulation in the solar system, which contains only one parameter the so-called solar-modulation  $\phi$ . Considering the charge-sign and suspected nuclei species dependence of the solar modulation which is represented in previous fitting [24], we adopt  $\phi_p$ ,  $\phi_{\text{He}}$ ,  $\phi_C$ ,  $\phi_O$ ,  $\phi_{\bar{p}}$ ,  $\phi_{\text{Li}}$ ,  $\phi_{\text{Be}}$ , and  $\phi_B$  to modulate the proton, He, C, O,  $\bar{p}$ , Li, Be, and B nuclei data, respectively. This would give us a limitation of force-field approximation as a simple and effective theory to describe the solar modulation on local interstellar spectra (LIS).

## 4. Numerical tools

The public code GALPROP v56<sup>1</sup> [28–32] was used to solve the diffusion equation numerically. In view of some discrepancies when fitting with the new data which use the default primary source (injection) isotopic abundances in GALPROP [33], we use factors  $c_{\text{He}}$ ,  $c_C$ , and  $c_O$  to re-scale the helium-4, carbon-12, and oxygen-16 abundance. At the same time,  $c_{\bar{p}}$ ,  $c_{\text{Li}}$ ,  $c_{\text{Be}}$ , and  $c_B$  are employed to re-scale the uncertainties from the  $\bar{p}$ , Li, Be, and B' production cross sections. Here, we expect that a constant factor is a simple assumption, which would help us to get a better fitting result.

## B. Data Sets and Parameters

In our work, the proton flux (from AMS-02 and CREAM [2, 4]), helium flux (from AMS-02 and CREAM [2, 5]), carbon flux (from AMS-02 [6]), oxygen flux (from AMS-02 [6]), anti-proton flux (from AMS-02 [34]), lithium flux (from AMS-02 [7]), beryllium flux (from AMS-02 [7]), and boron flux (from AMS-02 [7]) are added in the global fitting data set. The CREAM data is used as the supplement of the AMS-02 data because it is more compatible with the AMS-02 data when  $R \gtrsim 1$  TV. The errors used in our global fitting are the quadratic sum of statistical and systematic errors.

Altogether, the data set in our global fitting is

$$D = \{D_p^{\text{AMS-02}}, D_{\text{He}}^{\text{AMS-02}}, D_C^{\text{AMS-02}}, D_{\emptyset}^{\text{AMS-02}}, D_{\bar{p}}^{\text{AMS-02}}, D_{\text{Li}}^{\text{AMS-02}}, D_{\text{Be}}^{\text{AMS-02}}, D_B^{\text{AMS-02}}, D_p^{\text{CREAM}}, D_{\text{He}}^{\text{CREAM}}\}.$$

---

<sup>1</sup> <http://galprop.stanford.edu>

The parameter sets for Scheme I is

$$\boldsymbol{\theta}_1 = \{D_0, \delta, z_h, v_A, | \\ R_p, R_{p2}, \nu_{p1}, \nu_{p2}, \nu_{p3}, \\ R_{He1}, R_{He2}, \nu_{He1}, \nu_{He2}, \nu_{He3}, | \\ N_p, c_{He}, c_C, c_O, c_{\bar{p}}, c_{Li}, c_{Be}, c_B, | \\ \phi_p, \phi_{He}, \phi_C, \phi_O, \phi_{\bar{p}}, \phi_{Li}, \phi_{Be}, \phi_B\} ,$$

for Scheme II is

$$\boldsymbol{\theta}_2 = \{D_0, R_{br}, \delta_1, \delta_2, z_h, v_A, | \\ R_p, \nu_{p1}, \nu_{p2}, R_{He}, \nu_{He1}, \nu_{He2}, | \\ N_p, c_{He}, c_C, c_O, c_{\bar{p}}, c_{Li}, c_{Be}, c_B, | \\ \phi_p, \phi_{He}, \phi_C, \phi_O, \phi_{\bar{p}}, \phi_{Li}, \phi_{Be}, \phi_B\} .$$

These parameters can be separated into four groups: the propagation parameters, the source parameters, the modulation parameters and re-scale parameters. And their priors are chosen to be uniform distributions with the prior intervals given in Tables I and II.

### III. FITTING RESULTS

When the Markov Chains have reached their equilibrium states, we take the samples of the parameters as their posterior probability distribution function (PDF). The best-fitting results and the corresponding residuals of the primary nuclei flux for 2 schemes are showed in Fig. 1, and the corresponding results of the secondary nuclei flux are showed in Fig. 2.<sup>2</sup>

The best-fit values, statistical mean values, standard deviations and allowed intervals at 95% CL for parameters in set  $\boldsymbol{\theta}_1$  and  $\boldsymbol{\theta}_2$  are shown in Table I and Table II, respectively. For best-fit results of the global fitting, we got  $\chi^2/d.o.f = 383.45/521$  for Scheme I and  $\chi^2/d.o.f = 395.48/524$  for Scheme II.

### IV. DISCUSSIONS AND CONCLUSIONS

In this work, we use the newly released data from AMS-02 [4–7, 34], to study the origin of the spectra hardening in the primary (proton, helium, carbon and oxygen) and secondary (anti-proton, lithium, beryllium and boron) CR nuclei spectra based on 2 different schemes. Global fitting results have shown that, both of the schemes could give an effective fitting on the current primary and secondary nuclei spectra from AMS-02,

and could reproduce the hardening of the spectra obviously. More precise secondary nuclei data on high energy regions ( $\gtrsim 1$  TV) is needed to distinguish these two schemes.

In our global fitting, each kind of the species has employed an independent modulation potential  $\phi$  to account for the solar modulation, which is based on the force-field approximation. As a widely used and effective treatment on solar modulation, such configuration could show us the limitation of its effects. In most of the situations, it could give us an acceptant results.<sup>3</sup> If we want to study the fine structures in low-energy regions of the spectra ( $\lesssim 30$  GV), we should consider more effects in solving the Parker transport equation which contains diffusion, convection, particle drift and energy loss (see, e.g., Boschini et al. [35]). On the other hand, the different fitting values of  $\phi$  for different nuclei species indicate some of the species really experience different physical processes in the heliosphere. Especially for beryllium, it needs further researches.<sup>4</sup>

Another interesting aspect comes from the fitting values of the re-scale factors. All the primary nuclei abundance have a re-scale factor of  $0.5 \sim 0.6$ . We know that in GALPROP, the primary source (injection) isotopic abundances are taken first as the solar system abundances, which are iterated to achieve an agreement with the propagated abundances as provided by ACE at  $\sim 200$  MeV/nucleon [36, 37] assuming a propagation model. As a result, it is natural that the abundance of the CR species in the solar system (relatively low rigidity CR particles) is different from that of the outer space (relatively high rigidity CR particles). This provide us a effective and independent way to study the isotopic abundance out of the solar system. Moreover, all the re-scale factors of the secondary nuclei species are larger than 1.0, some of them can reach up to  $1.7 \sim 1.8$  ( $c_{\bar{p}}$  and  $c_{Be}$ ). Because these factors represent the re-scale on the production cross section of the species, this would lead to further study on these cross sections on colliders and would open a new door to study nuclear physics.<sup>5</sup>

**Note:** Excluding the fitting values of  $c_{\bar{p}}$  and  $\phi_{\bar{p}}$  for anti-proton's negative charge, we find that the most special species is beryllium, not only its propagation in heliosphere, but also the production cross section and isotopic abundance. This would be related to some interesting problems in stellar physics and cosmology on such this special element, which needs further research based on more precise CR data.

---

<sup>2</sup> Considering the correlations between different parameters, we could not get a reasonable reduced  $\chi^2$  for each part of the data set independently. As a result, we show the  $\chi^2$  for each part of the data set in Figs. 1, 2.

<sup>3</sup> Except the situation for anti-proton flux, it comes from the charge-sign dependence of the solar modulation, which cannot be handled by force-field approximation.

<sup>4</sup> Here we exclude another special species – anti-proton, whose particularity would mainly be generated by its negative charge.

<sup>5</sup> A such pioneering work can be found in Génolini et al. [38].

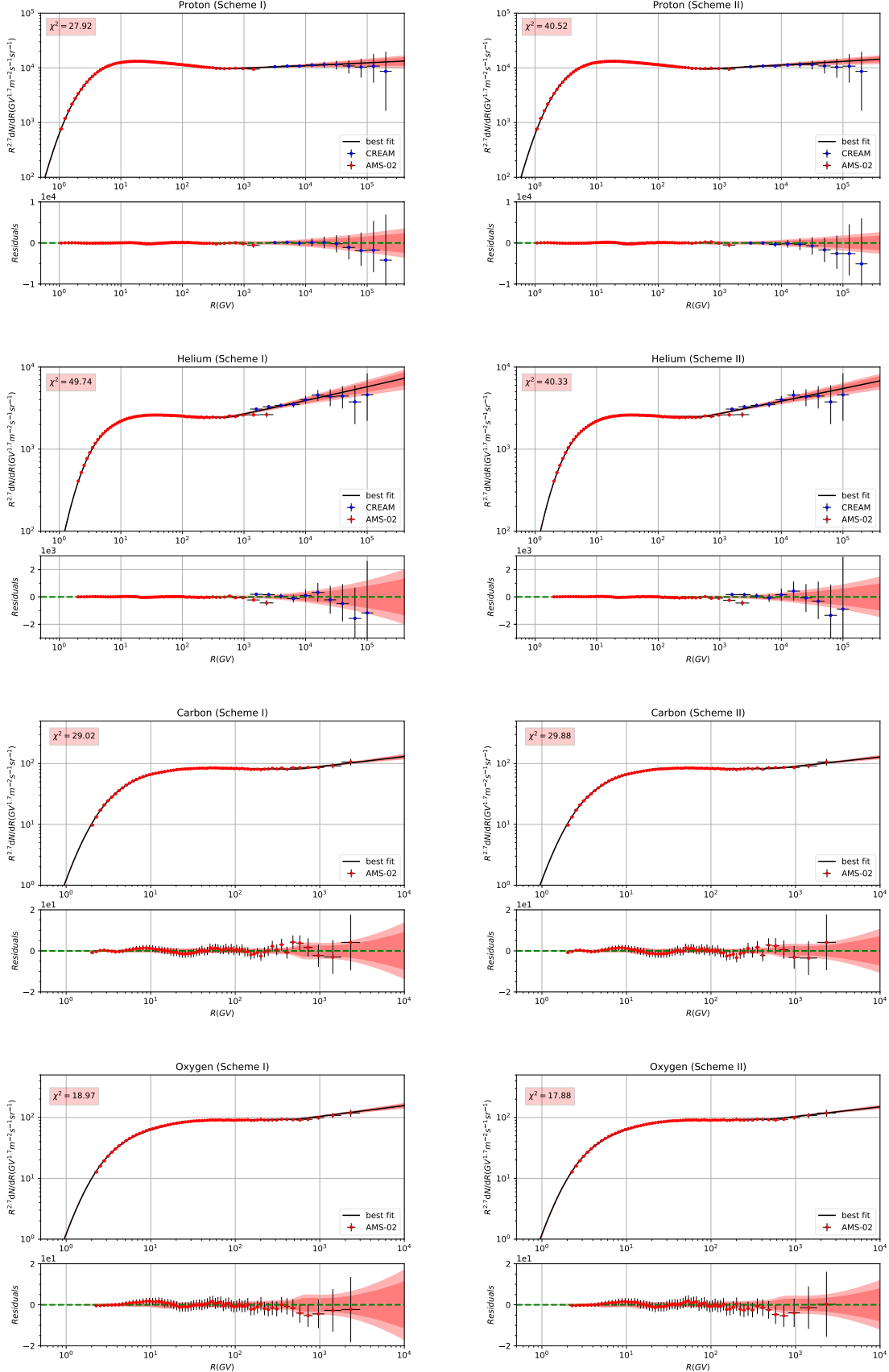


FIG. 1: The global fitting results and the corresponding residuals to the primary nuclei flux (proton flux, helium flux, carbon flux and oxygen flux) for 2 schemes. The  $2\sigma$  (deep red) and  $3\sigma$  (light red) bound are also showed in the figures.

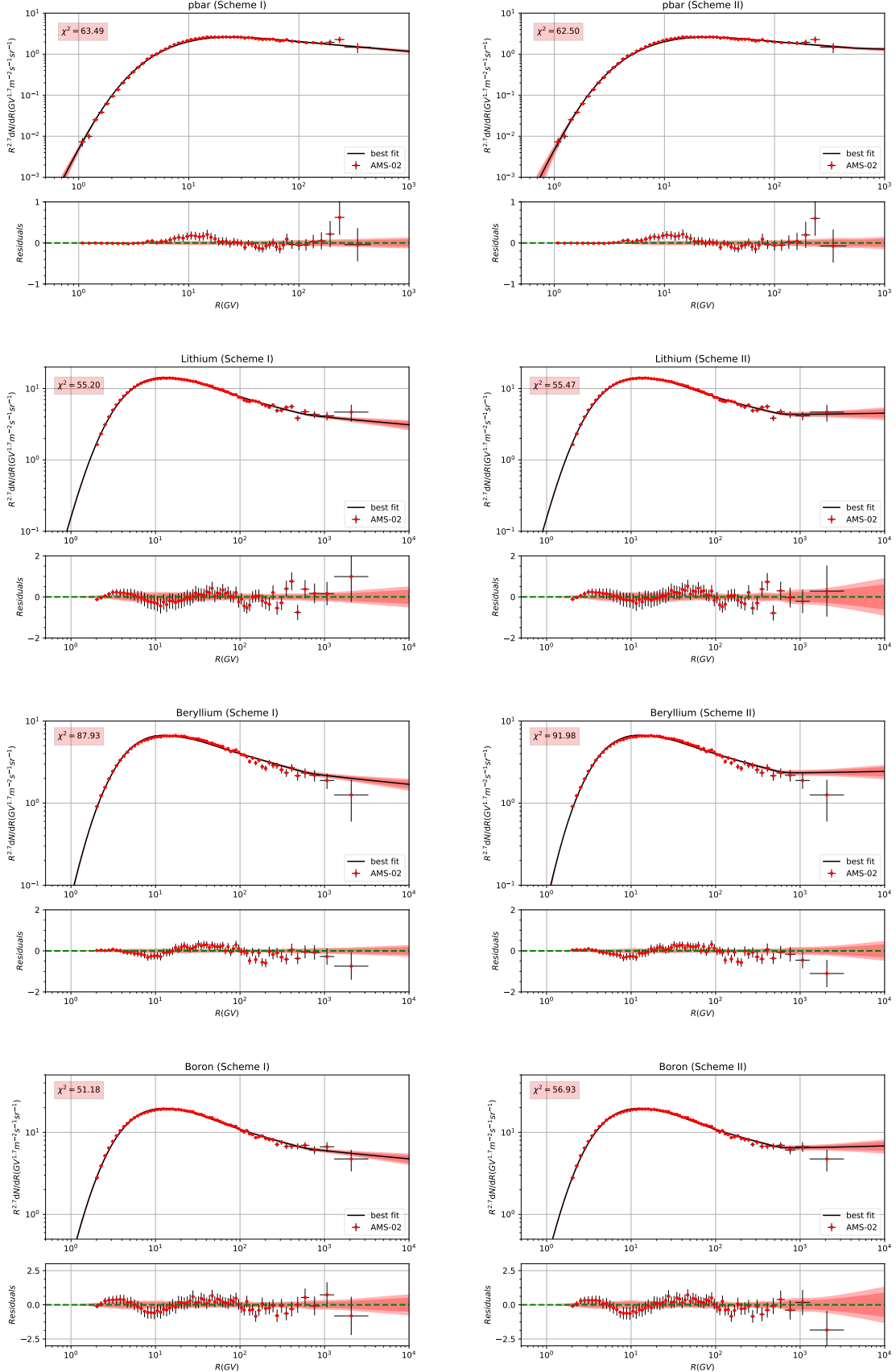


FIG. 2: The global fitting results and the corresponding residuals to the secondary nuclei flux (anti-proton flux, lithium flux, beryllium flux and boron flux) for 2 schemes. The  $2\sigma$  (deep red) and  $3\sigma$  (light red) bound are also showed in the figures.

ID	Prior range	Best-fit value	Posterior mean and Standard deviation	Posterior 95% range
$D_0$ ( $10^{28} \text{ cm}^2 \text{ s}^{-1}$ )	[1, 30]	18.36	$13.03 \pm 3.18$	[13.98, 20.92]
$\delta$	[0.1, 1.0]	0.28	$0.31 \pm 0.03$	[0.28, 0.30]
$z_h$ (kpc)	[0.5, 30.0]	11.30	$8.82 \pm 1.13$	[7.82, 12.31]
$v_A$ (km/s)	[0, 80]	56.89	$47.44 \pm 8.04$	[50.37, 62.26]
$R_{p1}$ (GV)	[1, 30]	24.61	$21.54 \pm 2.72$	[20.18, 26.22]
$R_{p2}$ (GV)	[60, 1000]	528.31	$640.23 \pm 87.56$	[486.96, 892.43]
$\nu_{p1}$	[1.0, 4.0]	2.18	$2.11 \pm 0.05$	[2.13, 2.20]
$\nu_{p2}$	[1.0, 4.0]	2.47	$2.46 \pm 0.02$	[2.46, 2.49]
$\nu_{p3}$	[1.0, 4.0]	2.37	$2.32 \pm 0.04$	[2.32, 2.38]
$R_{A1}$ (GV)	[1, 30]	22.23	$19.88 \pm 0.70$	[19.45, 23.41]
$R_{A2}$ (GV)	[60, 1000]	540.03	$413.85 \pm 87.40$	[394.88, 624.91]
$\nu_{A1}$	[1.0, 4.0]	2.10	$2.05 \pm 0.03$	[2.05, 2.11]
$\nu_{A2}$	[1.0, 4.0]	2.41	$2.40 \pm 0.01$	[2.40, 2.42]
$\nu_{A3}$	[1.0, 4.0]	2.25	$2.24 \pm 0.02$	[2.22, 2.28]
$N_p$ <sup>a</sup>	[1, 8]	4.45	$4.44 \pm 0.03$	[4.42, 4.49]
$c_{He}$	[0.1, 5.0]	0.64	$0.65 \pm 0.01$	[0.64, 0.65]
$c_C$	[0.1, 5.0]	0.55	$0.561 \pm 0.01$	[0.54, 0.56]
$c_O$	[0.1, 5.0]	0.50	$0.52 \pm 0.02$	[0.49, 0.52]
$c_{\bar{p}}$	[0.1, 5.0]	1.72	$1.54 \pm 0.17$	[1.57, 1.92]
$c_{Li}$	[0.1, 5.0]	1.43	$1.28 \pm 0.16$	[1.31, 1.58]
$c_{Be}$	[0.1, 5.0]	1.70	$1.55 \pm 0.15$	[1.57, 1.88]
$c_B$	[0.1, 5.0]	1.10	$1.01 \pm 0.10$	[1.02, 1.20]
$\phi_p$ (GV)	[0, 1.5]	0.70	$0.70 \pm 0.05$	[0.66, 0.75]
$\phi_{He}$ (GV)	[0, 1.5]	0.61	$0.65 \pm 0.05$	[0.56, 0.67]
$\phi_C$ (GV)	[0, 1.5]	0.72	$0.73 \pm 0.04$	[0.67, 0.78]
$\phi_O$ (GV)	[0, 1.5]	0.74	$0.72 \pm 0.04$	[0.68, 0.77]
$\phi_{\bar{p}}$ (GV)	[0, 1.5]	0.008	$0.25 \pm 0.26$	[0.001, 0.171]
$\phi_{Li}$ (GV)	[0, 1.5]	0.65	$0.74 \pm 0.12$	[0.56, 0.75]
$\phi_{Be}$ (GV)	[0, 1.5]	0.27	$0.41 \pm 0.13$	[0.20, 0.40]
$\phi_B$ (GV)	[0, 1.5]	0.63	$0.72 \pm 0.11$	[0.56, 0.74]

<sup>a</sup> Post-propagated normalization flux of protons at 100 GeV in unit  $10^{-2} \text{ m}^{-2} \text{ s}^{-1} \text{ sr}^{-1} \text{ GeV}^{-1}$

TABLE I: Constraints on the parameters in set  $\theta_1$ . The prior interval, best-fit value, statistic mean, standard deviation and the allowed range at 95% CL are listed for parameters. With  $\chi^2/d.o.f = 383.45/521$  for best fit result.

## ACKNOWLEDGMENTS

This research was supported in part by the Projects 11475238 and 11647601 supported by National Science Foundation of China, and by Key Research Program of Frontier Sciences, CAS. The calculation in this paper are supported by HPC Cluster of SKLTP/ITP-CAS.

- 
- [1] A. D. Panov, J. H. Adams, H. S. Ahn, G. L. Bashindzhyan, K. E. Batkov, J. Chang, M. Christl, A. R. Fazely, O. Ganel, R. M. Gunashringha, T. G. Guzik, J. Isbert, K. C. Kim, E. N. Kouznetsov, M. I. Panasyuk, W. K. H. Schmidt, E. S. Seo, N. V. Sokolskaya, J. W. Watts, J. P. Wefel, J. Wu, and V. I. Zatsepин, ArXiv Astrophysics e-prints (2006), astro-ph/0612377.
- [2] H. S. Ahn, P. Allison, M. G. Bagliesi, J. J. Beatty, G. Bigongiari, J. T. Childers, N. B. Conklin, S. Coutu, M. A. DuVernois, O. Ganel, J. H. Han, J. A. Jeon, K. C. Kim, M. H. Lee, L. Lutz, P. Maestro, A. Malinin, P. S. Marrocchesi, S. Minnick, S. I. Mognet, J. Nam, S. Nam, S. L. Nutter, I. H. Park, N. H. Park, E. S. Seo, R. Sina, J. Wu, J. Yang, Y. S. Yoon, R. Zei, and S. Y. Zinn, *Astrophys. J. Lett.* **714**, L89 (2010), arXiv:1004.1123 [astro-ph.HE].
- [3] PAMELA Collaboration, O. Adriani, G. C. Barbarino, G. A. Bazilevskaya, R. Bellotti, M. Boezio, E. A. Bogomolov, L. Bonechi, M. Bongi, V. Bonvicini, S. Borisov, and el al., *Science* **332**, 69 (2011), arXiv:1103.4055 [astro-ph.HE].

ID	Prior range	Best-fit value	Posterior mean and Standard deviation	Posterior 95% range
$D_0$ ( $10^{28} \text{ cm}^2 \text{ s}^{-1}$ )	[1, 30]	18.27	$13.28 \pm 3.49$	[7.97, 18.63]
$R_{\text{br}}$ (GV)	[200, 800]	541.73	$504.43 \pm 96.85$	[324.73, 665.23]
$\delta_1$	[0.1, 1.0]	0.28	$0.31 \pm 0.04$	[0.27, 0.38]
$\delta_2$	[0.1, 1.0]	0.14	$0.19 \pm 0.05$	[0.13, 0.30]
$z_h$ (kpc)	[0.5, 30.0]	8.53	$8.51 \pm 0.04$	[8.44, 8.58]
$v_A$ (km/s)	[0, 80]	65.66	$50.07 \pm 11.24$	[33.36, 67.14]
$R_p$ (GV)	[1, 30]	27.88	$24.22 \pm 3.16$	[18.06, 28.63]
$\nu_{p1}$	[1.0, 4.0]	2.20	$2.12 \pm 0.06$	[2.03, 2.20]
$\nu_{p2}$	[1.0, 4.0]	2.49	$2.46 \pm 0.03$	[2.42, 2.49]
$R_A$ (GV)	[1, 30]	20.71	$19.47 \pm 1.91$	[15.63, 21.68]
$\nu_{A1}$	[1.0, 4.0]	2.07	$2.03 \pm 0.05$	[1.94, 2.08]
$\nu_{A2}$	[1.0, 4.0]	2.41	$2.39 \pm 0.02$	[2.35, 2.41]
$N_p^a$	[1, 8]	4.49	$4.45 \pm 0.03$	[4.41, 4.50]
$c_{\text{He}}$	[0.1, 5.0]	0.64	$0.66 \pm 0.01$	[0.64, 0.68]
$c_C$	[0.1, 5.0]	0.55	$0.57 \pm 0.01$	[0.55, 0.59]
$c_O$	[0.1, 5.0]	0.50	$0.53 \pm 0.03$	[0.50, 0.58]
$c_{\bar{p}}$	[0.1, 5.0]	1.89	$1.56 \pm 0.23$	[1.22, 1.95]
$c_{\text{Li}}$	[0.1, 5.0]	1.53	$1.30 \pm 0.17$	[0.95, 1.57]
$c_{\text{Be}}$	[0.1, 5.0]	1.80	$1.57 \pm 0.16$	[1.33, 1.83]
$c_B$	[0.1, 5.0]	1.18	$1.02 \pm 0.11$	[0.82, 1.20]
$\phi_p$ (GV)	[0, 1.5]	0.73	$0.70 \pm 0.05$	[0.65, 0.79]
$\phi_{\text{He}}$ (GV)	[0, 1.5]	0.57	$0.59 \pm 0.05$	[0.53, 0.68]
$\phi_C$ (GV)	[0, 1.5]	0.69	$0.68 \pm 0.04$	[0.63, 0.76]
$\phi_O$ (GV)	[0, 1.5]	0.71	$0.67 \pm 0.04$	[0.59, 0.74]
$\phi_{\bar{p}}$ (GV)	[0, 1.5]	0.002	$0.20 \pm 0.25$	[0.002, 0.718]
$\phi_{\text{Li}}$ (GV)	[0, 1.5]	0.56	$0.66 \pm 0.15$	[0.51, 0.94]
$\phi_{\text{Be}}$ (GV)	[0, 1.5]	0.18	$0.31 \pm 0.17$	[0.13, 0.66]
$\phi_B$ (GV)	[0, 1.5]	0.56	$0.63 \pm 0.11$	[0.51, 0.85]

<sup>a</sup> Post-propagated normalization flux of protons at 100 GeV in unit  $10^{-2} \text{ m}^{-2} \text{ s}^{-1} \text{ sr}^{-1} \text{ GeV}^{-1}$

TABLE II: Constraints on the parameters in set  $\theta_2$ . The prior interval, best-fit value, statistic mean, standard deviation and the allowed range at 95% CL are listed for parameters. With  $\chi^2/d.o.f = 395.48/524$  for best fit result.

- [4] AMS Collaboration, M. Aguilar, D. Aisa, B. Alpat, A. Alvino, G. Ambrosi, K. Andeen, L. Arruda, N. Attig, P. Azzarello, A. Bachlechner, and et al., Physical Review Letters **114**, 171103 (2015).
- [5] AMS Collaboration, M. Aguilar, D. Aisa, B. Alpat, A. Alvino, G. Ambrosi, K. Andeen, L. Arruda, N. Attig, P. Azzarello, A. Bachlechner, and et al., Physical Review Letters **115**, 211101 (2015).
- [6] M. Aguilar, L. Ali Cavasonza, B. Alpat, G. Ambrosi, L. Arruda, N. Attig, S. Aupetit, P. Azzarello, A. Bachlechner, F. Barao, and et al. (AMS Collaboration), Phys. Rev. Lett. **119**, 251101 (2017).
- [7] M. Aguilar, L. Ali Cavasonza, G. Ambrosi, L. Arruda, N. Attig, S. Aupetit, P. Azzarello, A. Bachlechner, F. Barao, and et al. (AMS Collaboration), Phys. Rev. Lett. **120**, 021101 (2018).
- [8] M. Korsmeier and A. Cuoco, ArXiv e-prints (2016), arXiv:1607.06093 [astro-ph.HE].
- [9] M. J. Boschini, S. Della Torre, M. Gervasi, D. Grandi, G. Jóhannesson, M. Kachelriess, G. La Vacca, N. Masi, I. V. Moskalenko, E. Orlando, S. S. Ostapchenko, S. Pennotti, T. A. Porter, L. Quadrani, P. G. Rancoita, D. Rozza, and M. Tacconi, Astrophys. J. **840**, 115 (2017), arXiv:1704.06337 [astro-ph.HE].
- [10] J.-S. Niu, T. Li, R. Ding, B. Zhu, H.-F. Xue, and Y. Wang, Phys. Rev. D **97**, 083012 (2018), arXiv:1712.00372 [astro-ph.HE].
- [11] J.-S. Niu, T. Li, and F.-Z. Xu, ArXiv e-prints (2017), arXiv:1712.09586 [hep-ph].
- [12] C.-R. Zhu, Q. Yuan, and D.-M. Wei, Astrophys. J. **863**, 119 (2018), arXiv:1807.09470 [astro-ph.HE].
- [13] Y. Génolini, P. D. Serpico, M. Boudaud, S. Caroff, V. Poulin, L. Derome, J. Lavalle, D. Maurin, V. Poireau, S. Rosier, P. Salati, and M. Vecchi, Physical Review Letters **119**, 241101 (2017).
- [14] P. Blasi, E. Amato, and P. D. Serpico, Physical Review Letters **109**, 061101 (2012), arXiv:1207.3706 [astro-ph.HE].
- [15] N. Tomassetti, Astrophys. J. Lett. **752**, L13 (2012), arXiv:1204.4492 [astro-ph.HE].
- [16] N. Tomassetti, Astrophys. J. Lett. **815**, L1 (2015), arXiv:1511.04460 [astro-ph.HE].
- [17] N. Tomassetti, Phys. Rev. D **92**, 081301 (2015), arXiv:1509.05775 [astro-ph.HE].
- [18] J. Feng, N. Tomassetti, and A. Oliva, Phys. Rev. D **94**, 123007 (2016), arXiv:1610.06182 [astro-ph.HE].
- [19] Y.-Q. Guo and Q. Yuan, Phys. Rev. D **97**, 063008 (2018), arXiv:1801.05904 [astro-ph.HE].

- [20] A. E. Vladimirov, G. Jóhannesson, I. V. Moskalenko, and T. A. Porter, *Astrophys. J.* **752**, 68 (2012), arXiv:1108.1023 [astro-ph.HE].
- [21] G. Bernard, T. Delahaye, Y.-Y. Keum, W. Liu, P. Salati, and R. Taillet, *Astron. Astrophys.* **555**, A48 (2013), arXiv:1207.4670 [astro-ph.HE].
- [22] S. Thoudam and J. R. Hörandel, *Mon. Not. Roy. Astron. Soc.* **435**, 2532 (2013), arXiv:1304.1400 [astro-ph.HE].
- [23] N. Tomassetti and F. Donato, *Astrophys. J. Lett.* **803**, L15 (2015), arXiv:1502.06150 [astro-ph.HE].
- [24] J.-S. Niu and T. Li, *Phys. Rev. D* **97**, 023015 (2018), arXiv:1705.11089 [astro-ph.HE].
- [25] Q. Yuan, S.-J. Lin, K. Fang, and X.-J. Bi, ArXiv e-prints (2017), arXiv:1701.06149 [astro-ph.HE].
- [26] Q. Yuan, C.-R. Zhu, X.-J. Bi, and D.-M. Wei, ArXiv e-prints (2018), arXiv:1810.03141 [astro-ph.HE].
- [27] L. J. Gleeson and W. I. Axford, *Astrophys. J.* **154**, 1011 (1968).
- [28] A. W. Strong and I. V. Moskalenko, *Astrophys. J.* **509**, 212 (1998), astro-ph/9807150.
- [29] I. V. Moskalenko, A. W. Strong, J. F. Ormes, and M. S. Potgieter, *Astrophys. J.* **565**, 280 (2002), astro-ph/0106567.
- [30] A. W. Strong and I. V. Moskalenko, *Advances in Space Research* **27**, 717 (2001), astro-ph/0101068.
- [31] I. V. Moskalenko, A. W. Strong, S. G. Mashnik, and J. F. Ormes, *Astrophys. J.* **586**, 1050 (2003), astro-ph/0210480.
- [32] V. S. Ptuskin, I. V. Moskalenko, F. C. Jones, A. W. Strong, and V. N. Zirakashvili, *Astrophys. J.* **642**, 902 (2006), astro-ph/0510335.
- [33] G. Jóhannesson, R. Ruiz de Austri, A. C. Vincent, I. V. Moskalenko, E. Orlando, T. A. Porter, A. W. Strong, R. Trotta, F. Feroz, P. Graff, and M. P. Hobson, *Astrophys. J.* **824**, 16 (2016), arXiv:1602.02243 [astro-ph.HE].
- [34] AMS Collaboration, M. Aguilar, L. Ali Cavasonza, B. Alpat, G. Ambrosi, L. Arruda, N. Attig, S. Aupetit, P. Azarelo, A. Bachlechner, F. Barao, and et al., *Physical Review Letters* **117**, 091103 (2016).
- [35] M. J. Boschini, S. Della Torre, M. Gervasi, G. La Vacca, and P. G. Rancoita, ArXiv e-prints (2017), arXiv:1704.03733 [astro-ph.SR].
- [36] M. E. Wiedenbeck, N. E. Yanasak, A. C. Cummings, A. J. Davis, J. S. George, R. A. Leske, R. A. Mewaldt, E. C. Stone, P. L. Hink, M. H. Israel, M. Lijowski, E. R. Christian, and T. T. von Rosenvinge, *Space Sci. Rev.* **99**, 15 (2001).
- [37] M. E. Wiedenbeck, W. R. Binns, A. C. Cummings, G. A. de Nolfo, M. H. Israel, R. A. Leske, R. A. Mewaldt, R. C. Ogiore, E. C. Stone, and T. T. von Rosenvinge, *International Cosmic Ray Conference* **2**, 149 (2008).
- [38] Y. Génolini, D. Maurin, I. V. Moskalenko, and M. Unger, *Phys. Rev. C* **98**, 034611 (2018), arXiv:1803.04686 [astro-ph.HE].